Pressure and Velocity in a Developing Coaxial Jet

L. F. Moon
Textron Bell Aerospace, Buffalo, New York

Determinations of static pressure, mean velocity and turbulence intensity in the developing region of coaxial jets are presented. Detailed profiles were obtained at twelve axial locations (extending from the nozzle exit for a distance of 5 diameters) downstream from a single element of the Bell Aerospace H_2/O_2 19-element coaxial injector. Measurements of mass-flux per unit area (using a constant temperature anemometer), total pressure and local temperature were used in the determination of local static pressure and velocity. These data show a low pressure region exists near the nozzle exit. Although this pressure reduction is small (0.34 psi), it substantially altered the flow development. Comparison of results shows that velocity near the nozzle exit decreases initially (no central velocity core) as a result of both pressure gradients and viscous mixing. These data are compared with analytical predictions made using available computer codes. Results show the need to consider pressure effects in any proposed mathematical model.

Nomenclature

A = area
M = Mach number
P = pressure
R = gas constant
Re = Reynolds number
T = temperature
$\bar{U}$ = mean velocity
$\sqrt{u^2}$ = rms velocity
$\bar{V}$ = indicated mean velocity (hot film)
ρ = density
γ = ratio of specific heats

Subscripts

c = during calibration
i = inner nozzle
o = outer annulus/total pressure or temperature

Introduction

THE measurements described herein are concerned with the developing region of coaxial injector where the exit velocity of the inner nozzle is significantly less than that of the annulus. The motivation for this investigation was twofold. First, because coaxial elements form the basic injection mechanism for many combustors, it was of interest to better characterize the initial flow region of such elements. Second, since computations for reaction systems are often based on the ability to predict the non-reactive turbulent mixing, it was also of interest to characterize such a flow in detail and compare the results with predictions made using available computational techniques.

In combustors employing diffusion flames, the kinetics of the reaction are rapid and the rate of reaction is controlled by the turbulent mixing. Several experimental investigations have been conducted in the mixing region of coaxial jets. Investigations of the mean velocity field of coaxial jets using pitot tubes are discussed.[1-3] Two more recent investigations have been conducted using hot wire anemometers to measure both the mean and turbulence structure of the flow.[4,5] One assumption, which seems to be common to these investigations is that the static pressure gradients in the developing region of the flow are small and can be neglected. For velocity ratios, U_0/U_i, greater than one and area ratios, A_1/A_i, greater than zero (typical of real combustors), neglecting differences in static pressure may not be a good assumption. When using total and static pressure data to calculate mean velocity for incompressible flows, even extremely small changes in static pressure can cause large errors in the velocity determined. These small changes in static pressure do not, however, cause large errors in velocity measured using a hot wire. Using hot wire anemometry, both Champagne and Wygnanski,[4] and Durao and Whitelaw,[5] investigated incompressible coaxial flows where the velocity ratios were greater than one. The measurements of Champagne and Wygnanski were concerned with the developing region of coaxial jets where the initial flows were nearly fully potential and separated by a negligible distance. In contrast, the measurements of Durao and Whitelaw were for fully developed flows with a significant separation distance.

The present study is concerned with the flow from a coaxial injector element from an actual combustor. As with most practical flow hardware, the nozzle and annulus flows were neither fully potential nor fully developed and the separation distance (splitter plate) was relatively large. Measurements were made for a velocity ratio greater than one and in contrast to previous investigations the velocities were in the compressible range. These higher velocities are typical of real combustors, e.g.,[6-9].

Experimental Procedure

In this experimental investigation, a Bell 19-element coaxial injector, which had been previously tested during hot firings, was selected and all elements except the central one were masked. A photograph of this injector, geometrical shape and physical size are shown in Fig. 1. Note, that the splitter plate separating the central jet and annulus was recessed 0.03 in. from the injector face. The constant area inlet length was about 6 diameters for the central nozzle and about 7 nozzle thickness for the annulus. Therefore, fully developed turbulent flow conditions were not expected at the injector exit. The area ratio between the annulus and nozzle, A_0/A_i, was 1.48 and the ratio of the splitter base area to the central nozzle, A_1/A_i, was 1.02. The ratio of the annulus velocity ($\bar{U}=700$ fps) to that of the central jet ($\bar{U}=250$ fps) was equal to 2.8 for all tests. These velocities and dimensions correspond to Reynolds numbers of 3.8×10^5 based on diameter for the inner jet and 2.0×10^6 based on annulus height for the outer jet and are approximately one order of magnitude larger than those previously investigated.[4,5]

Received October 24, 1974; revision received June 6, 1975. The author wishes to express his thanks to Dr. J. H. Morgenthaler for his many discussions and suggestions. He would also like to express his thanks to Dr. Richard J. Priem, NASA-Lewis, for suggesting this investigation of a real injector element. This work was supported by NASA-Lewis Research Center, Contract NAS3-16798.

Index categories: Jets, Wakes, and Viscid-Inviscid Flow Interactions; Nozzle and Channel Flow; Rocket Engine Testing.

*Principal Scientist, Experimental Fluid Mechanics.

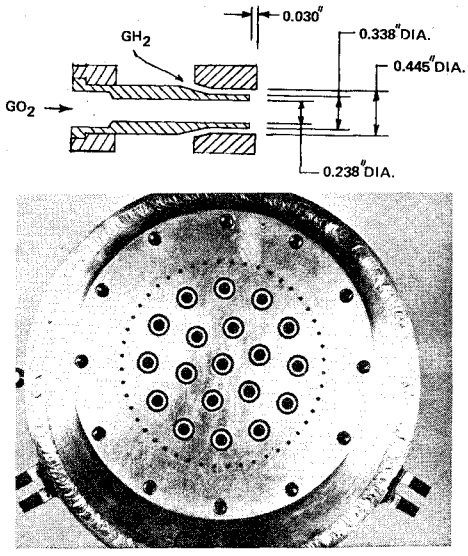

Fig. 1 Bell 19 element gaseous injector.

In these experiments, clean, dry compressed air was supplied at constant pressure and temperature to the two plenum chambers. Plenum pressure was measured on a mercury manometer for the high velocity outer jet and on a precision pressure indicator (TI-145) for the low velocity inner jet. Both plenum and room temperature were maintained at $70 \pm 1°F$ during all tests.

Measurements of mean velocity and turbulence intensity were made using a linearized constant temperature anemometer (TSI-1050). The hot film probe (TSI-1270-10) was calibrated and linearized to 2% of reading over the range 100-700 fps. Below 100 fps the error increased becoming about 4% at 50 fps. To assure calibration accuracy, the zero and maximum velocity points were checked before measurements were made at each axial station. The mean value of the linearized signal was determined using a true integrator (DISA-52B30) and displayed on a digital voltmeter (Fluke-8200A). The rms signal was obtained from a true rms meter (TSI-1060).

Total pressure measurements were made using a pitot probe fabricated from a 0.020 in o.d. by 0.004 in. wall stainless steel tube with the tip flattened to 0.006 in. inside and ground to 0.010 in. outside height. Pitot pressure was sensed using a precision pressure indicator (TI-145) which was calibrated and shown to have inaccuracies less than ± 0.001 psid at the 3 sigma level of confidence. Atmospheric pressure was measured using a similar instrument which had inaccuracies less than ± 0.004 psia at the 3 sigma level.

Surveys of the flowfield were made by mounting the coaxial injector on a translating table (mill bed) and moving the injector relative to a fixed probe position. By driving the gears of the translating table in only one direction, the displacement of the test nozzle was known accurately to ± 0.001 in. Initial location of the probes relative to the coaxial injector was determined using a theodolite.

Detailed velocity and pressure measurements were made along the jet centerline beginning 0.010 in. downstream of the nozzle exit and continuing for 2.50 in. Axial stations at which velocity profiles were obtained are 0.010, 0.030, 0.075, 0.15, 0.25, 0.50, 0.75, 1.00, 1.25, 1.50, 2.00, and 2.50 in. Pressure profiles were obtained at three axial stations: 0.010, 0.10, and 0.25 in.

Qualitative Description of Coaxial Jet Mixing

It is helpful in understanding these results to form a picture of the developing flowfield. Some of the flow parameters which must be considered are Reynolds numbers, velocity and area ratios, and the state of the flow, i.e., fully viscous or potential-like flow. In forming a picture of the flow, first consider conditions where the Reynolds numbers and velocity ratio are high ($Re_0 > Re_i > 10^4$, $U_0/U_i > 1$) and where the area of the splitter plate to that of the central nozzle is extremely small, i.e., where the thickness of the plate separating the inner from the outer flow can be neglected, $A_l/A_i \approx 0$. For these conditions and completely viscous flow at the injector exit, velocity at the nozzle centerline must increase due to viscous mixing between the high velocity outer jet and the low velocity inner jet. However, for a condition of potential-like flow at the injector exit, velocity along the centerline will remain constant until viscous mixing at the boundary between the two jets has had time to reach the centerline. In other words, a potential core will initially exist the length of which is dependent on both velocity and area ratios as well as the initial thickness of the boundary layers at the nozzle exit. An example of this type of flow is discussed in the paper by Champaign and Wygnanski.[4]

Now consider for a moment the same flow conditions as above except let the splitter plate have a finite thickness, $A_l/A_i \approx 1$. The flow must now expand to fill the region immediately downstream of this plate. Therefore, a recirculation region will develop which contains two vortices of opposite direction of rotation, Fig. 2. This recirculation region has approximately the same thickness as the splitter plate at the nozzle exit and tapers to zero at some downstream point. For the condition of a thick splitter plate, as opposed to a negligible one, the momentum transfer is initially from both jets into the recirculation region instead of from the high speed outer jet directly to the low speed inner one. Downstream where the recirculation zone ends, the momentum exchange is again from the outer to the inner jet and the centerline velocity will now begin to increase. An example of fully developed jet mixing with a finite splitter plate is discussed in the paper by Durao and Whitelaw.[5]

The velocity decay in the early developing region of the flow, the region contained within the recirculation zone, is caused by at least two separate mechanisms: viscous mixing and pressure gradients. To help in understanding the separate effects each of these mechanisms has on the flow development, consider again the flow condition shown in Fig. 2, but in contrast to the earlier example consider the flow at the nozzle exit to the potential with only a thin viscous region at its boundary. If the static pressure were constant everywhere downstream of the nozzle, as in a free jet, then viscous mixing would cause a decrease in velocity near the jet edge but a potential core would exist near the center, i.e., the centerline velocity would remain constant for a short distance downstream. The static pressure is, however, not constant throughout the flow. For conditions where the splitter plate is not negligible, the recirculation zone forms a pseudo-diffuser, causing a low pressure region to exist near the nozzle exit. Within this region, lines of constant mass diverge and even for potential-like flow velocity decreases almost uniformly across the jet. Viscous effects, which are always present, cause a slightly more rapid decrease in velocity at the jet boundary. For potential flow, where the viscous mixing region at the jet boundary has not spread to the centerline by the time the flow reaches the end of the recirculation zone, the velocity at the centerline will, after leaving the zone, remain constant until viscous effects reach the center.

Experimental Results

Due to physical limitations, flows in practical injectors are neither completely potential nor fully developed at the nozzle exit. Experimentally determined initial velocity profiles for one element of the Bell 19-element injector are shown in Fig. 3. In this same figure are power law curves representing a state of fully viscous initial flow. Empirical fits, using experimental data,[10] show that a 1/7th power law gives the best

agreement for Reynolds numbers near 3.8×10^5 and that a 1/10th power works best for Reynolds numbers near 2.0×10^6. A comparison of these curves with the measurements indicates that the flow was not fully developed. Note that a small potential-like region exists near the center of each jet.

An overlay of velocity profiles measured at twelve axial locations is shown in Figs. 4 and 5. Before discussing these data, several comments should be made regarding the hot film used and it sensitivity. First, the power dissipated by the air passing over the heated film depends on both the mass flow rate past the sensor and the temperature difference between the sensor and fluid. Where this temperature difference is held constant, as it was during these measurements, the hot film is primarily sensitive to the fluid mass flow per unit area ρU. For measurements made at the same flow conditions for which a sensor is calibrated, velocity can be determined directly; however, for measurements made at conditions other than those for which it was calibrated, a correction for density must be made. The actual velocity is thus equal to the indicated velocity times the density during calibration divided by the density of the flow being measured, $U=V\rho_c/\rho$. Second, cylindrical hot films are sensitive to flow velocity normal to their axis and almost insensitive to any velocity components along their axis. These films are, moreover, not sensitive to the direction of flow normal to their axis, i.e., the magnitude of the velocity component normal to the axis is measured and not its direction. Thus, measurements in regions of flow recirculation will be incorrect.

The profiles presented in Fig. 4 show a rapid velocity decrease in the initial region of the central jet owing to both viscous and pressure effects. If the initial velocity at the nozzle centerline is considered potential, Fig. 3, the decrease in velocity between stations $z=0.010$ in. and 0.075 in. must be to a large extent due to pressure effects. Evidence of strong viscous effects can also be seen by noting the much more rapid decrease in velocity at the jet boundary when going from $z=0.01$ to 0.15 in. This figure indicates that for $z\leqslant0.25$ in. the momentum exchange is from both the inner and outer jets into the recirculation zone behind the splitter plate. Somewhere between $z=0.25$ and $z=0.50$ in. the recirculation zone ends and the momentum transfer is from the high velocity annulus flow directly to the lower velocity inner jet. Also, illustrated by this figure is the tendency for the higher speed annulus flow to collapse around the central jet. A comparison of the peak velocity at $z=0.15$, 0.25, and 0.50 in. shows these peaks to be moving toward the nozzle centerline. Figure 5 shows this trend to continue until the flow becomes jet like somewhere between $z=1.5$ and 2.0 in. It is also evident from this figure that the velocity near the outer edge of annulus flow, $r\approx\pm0.22$ in., remains almost constant until the flow becomes jet-like, at which time the velocity across the entire flowfield decays with distance. This is seen by nothing that the profiles measured at all stations except $z=2.5$ in., cross at approximately the same point.

To qualify the importance of pressure gradients in the initial region of the flow, a measure of static pressure was needed. Because direct measurements of static pressure are difficult, if not impossible to make near the exit of such a small injector, an indirect measure was made. In contrast to static pressure, total pressure can be accurately measured for the flow conditions considered here. Measurements of total pressure P_0 in addition to mass flux per unit area $\rho\bar{U}$ and total temperature T_0 are sufficient to evaluate local static pressure. Static pressure at a point can for an ideal gas be written in terms of the local total pressure and Mach number as

$$P_0/P=[1+((\gamma-1)/2)M^2]^{\gamma/\gamma-1} \qquad (1)$$

where Mach number is defined by

$$M^2=\rho\bar{U}^2/\gamma P$$

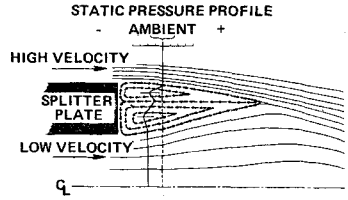

Fig. 2 Sketch of flow around splitter plate for high velocity outer and low velocity inner jets.

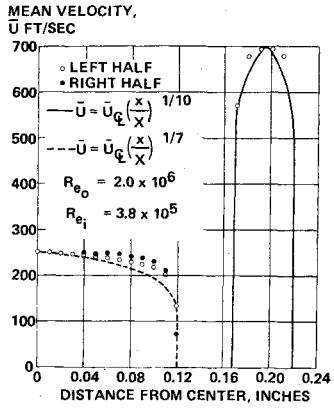

Fig. 3 Comparison of initial velocity profiles with 1/7 and 1/10 power laws.

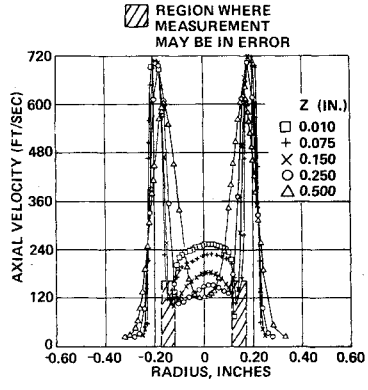

Fig. 4 Comparison of mean velocity profiles for $0.01\leqslant Z\leqslant0.5$.

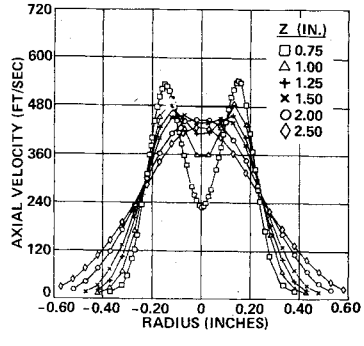

Fig. 5 Comparison of mean velocity profiles for $0.75\leqslant Z\leqslant2.5$.

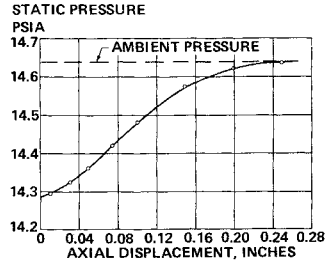

Fig. 6 Centerline static pressure vs axial displacement.

Mach number can be rewritten in terms of velocity measured using the hot film, $\bar{U}=\rho_c \bar{V}/\rho$, and static pressure as

$$M^2 = \frac{V^2}{\gamma R T_0}\left[\frac{P_c}{P}\,\frac{T}{T_c}\right]^2\left[1+\frac{\gamma-1}{2}M^2\right] \qquad (2)$$

Where the flow static temperature is equal to the static temperature during calibration Eqs. (1) and (2) can be simultaneously solved for static pressure.

The effect of experimental error when evaluating static pressure can most easily be seen by expanding Eq. (1) for small Mach number.

$$P_0/P = 1+\gamma M^2/2+\gamma M^4/8+\ldots.$$

By substituting Eq. (2) for M^2 and neglecting temperature differences one gets a quadratic equation for static pressure, which when solved becomes

$$P=\frac{1}{2\left(1+\dfrac{\gamma M^4}{8}+\ldots\right)}\left\{P_0+\left[P_0^2-\frac{2P_c^2}{RT_0}\bar{V}^2\left[1+\frac{\gamma-1}{2}M^2\right]\left[1+\frac{\gamma M^4}{8}+\ldots\right]\right]\right\}^{1/2}$$

During this investigation, the central jet Mach number was always less than 0.23, therefore, the terms $(\gamma-1)M^2/2$, $\gamma M^4/8$ and higher order terms were neglected and the previous equation differentiated to give a simple expression relating static pressure error to errors in measurements of mean velocity and total pressure.

$$\frac{dP}{P}=\left[\frac{|dP_0|}{P_0}+\frac{|d\bar{V}|}{\bar{V}}\right]\times\left[1-\frac{2P_c^2\bar{V}^2}{P_0^2RT_0}\right]^{-1/2}-\left|\frac{d\bar{V}}{\bar{V}}\right| \qquad (3)$$

Evaluation of Eq. (3) for errors of 2% in $\bar{V}$ and 0.25% in P_0 show the expected error in static pressure to be less than 0.4%.

Using the hot film and pitot tube data and Eq. (1) and (2), static pressure was determined. The data plotted in Fig. 6 shows static pressure to be approximately 2.5% below ambient at the nozzle exit (14.30 psia compared to 14.64 psia), to increase rapidly and become equal to ambient just beyond $z=0.25$ in. (approximately one inner nozzle diameter). Shown in Fig. 7 are three radial pressure profiles. The profiles measured at $z=0.01$, 0.10 and 0.25 in. show static pressure across the central jet boundary for $z=0.01$ in. These figures show axial pressure gradients to be much stronger than the radial ones for the flow contained within the central jet. However, outside this region, in the recirculation zone, radial pressure gradients must be very steep because it is across this very narrow region that the pressure increases to read ambient. No pitot tube data were taken in this recirculation region since such data would be subject to large experimental errors.

Discussion

Figure 8 has been prepared to show that the static pressure measured at the nozzle exit is of the magnitude one should expect. Shown in this figure is a plot of inner nozzle exit pressure as a function of annulus plenum pressure. With no

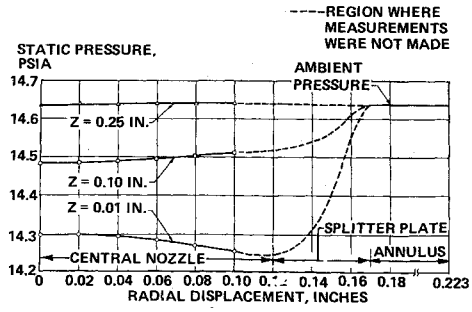

Fig. 7 Radial static pressure profiles.

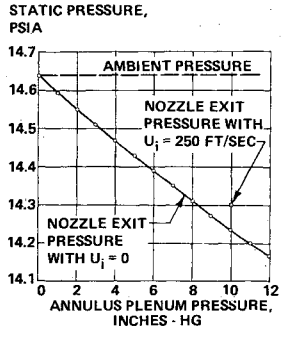

Fig. 8 Pressure at injector exit vs annulus plenum pressure.

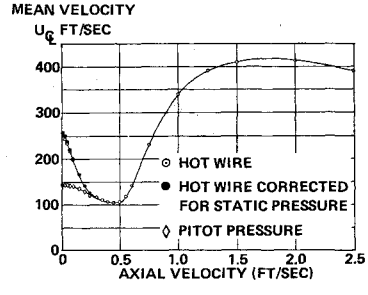

Fig. 9 Centerline velocity vs axial displacement.

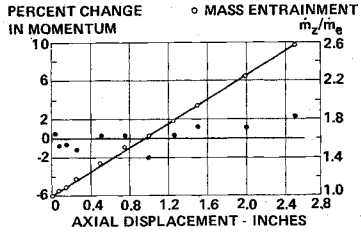

Fig. 10 Percent change in momentum; and variation of mass and momentum with axial displacement.

flow in the central jet, increasing velocity in the annulus causes a nearly linear decrease in pressure at the nozzle exit. Also shown in this figure is one static pressure point measured for an inner jet velocity of 250 fps and an annulus velocity of 700 fps (plenum pressure $\approx$ 10 in. Hg). As expected, the pressure was lowest with no flow in the nozzle and increased with increasing velocity.

Assuming that flow downstream of the splitter plate forms a pseudo-diffuser, one can by integration of the data given in Figs. 4-6 establish contours (lines) within which mass is constant and equal to the total flow through the central nozzle. Doing this, one finds that the flow expands approximately 60% of the distance across the splitter plate by the time pressure gradients disappear.

Effects of neglecting pressure gradients when evaluating velocity from hot film and pitot tube data can be seen in Fig. 9. Three separate curves of centerline velocity are shown. The velocity curve indicated by open circles is evaluated from hot film data directly while the curve indicated by solid circles is the same data corrected for changes in density (true velocity).

Comparison of these curves shows the maximum error in velocity due to neglecting density variations to be less than 3%. The third curve, indicated by diamonds, shows the velocity calculated directly from the total pressure data assuming static pressure everywhere equal to ambient (as is often done is reduction of pitot tube data for coaxial jets). Determination of velocity in this way can result in tremendous errors, e.g., the 2.5% difference in static pressure results in a difference of approximately 40% in calculated velocity. This large error results from taking the difference between pressure ratio and one, in contrast to hot wire errors which results from pressure ratio only.

Figure 9 shows not only a rapid decrease in centerline velocity due to both viscous and pressure effects ($z<0.35$ in), it also indicates a short region beyond the recirculation zone where the velocity remains constant (0.35 in. $<z<0.55$ in.). The reason for this, as has already been explained, is that the growing viscous region has not spread to the centerline before the flow leaves the recirculation zone. The sharp increase in velocity for $z>0.55$ in. shows that viscous effects have finally reached the centerline. Beyond $z\approx0.35$ in. and until the flow becomes jet-like at $z\approx2.0$ in., the momentum exchange is directly from the high velocity annulus flow to the lower velocity nozzle flow. There is, of course, during the entire flow development, a viscous region growing at the outer edge of the annulus. Where the ratio of annulus area to central nozzle area, $A_0/A_i>1$, which is the condition considered in this paper, the effect of this viscous region is to cause the flow to become jet-like more rapidly.[4]

To demonstrate the accuracy of the velocity measurements, momentum was calculated at each axial measuring station. The percent deviation in momentum from the mean of all measuring stations is shown as a function of axial displacement in Fig. 10. The maximum error over the entire measuring region is less than 2%. Two factors contributing to this small error are the nonlinearity of the hot film response and the finite region over which the momentum integral could be evaluated (the region over which measurements were made). Using these data, the rate of mass entrainment was determined. It is apparent, Fig. 10, that the rate of entrainment remains almost constant with downstream distance. Comparing this rate with that of a free jet, e.g., see Spalding[11], the coaxial injector corresponds to a free jet with nozzle diameter of 0.27 in. This is smaller than the annulus diameter (0.44 in) and larger than the central nozzle diameter (0.24 in), thus, the measured entrainment rate is within the expected range.

In addition to mean velocity, axial turbulence intensity was determined at each measuring station. Figure 11 shows an overlay of the velocity fluctuation profiles measured at 4 axial stations. During the early development, 3 intensity peaks exist, two corresponding to the mixing regions between the recirculation zone and the jets and one corresponding to the mixing regions at the outer edge of the annulus. The two peaks downstream of the splitter plate rapidly merge and become one at the end of the recirculation zone. Note that beyond this zone the inner peak decays and moves toward the centerline, becoming jet-like between $z=1.5$ and 2.0 in. In contrast, the outer peak remains at a fixed position, $z\approx0.22$ in., while decreasing in magnitude (as for a free jet). The change in magnitude of rms velocity intensity along the jet centerline can best be seen from Fig. 12. The rms velocity increases almost linearly with distance from the nozzle exit to the end of the region of recirculation, $z<0.25$ in. For a short distance outside this region, $0.25<z<0.45$ in., the intensity remains fairly constant then increases similar to the mean velocity. These regions of similarity, between the centerline mean velocity and rms velocity, do not coincide with one another however. Shown in Fig. 12 are two additional curves—one for mean velocity and another for the ratio of rms-to-mean velocity (turbulence intensity). Each of these curves show regions of rapid change in the flow properties

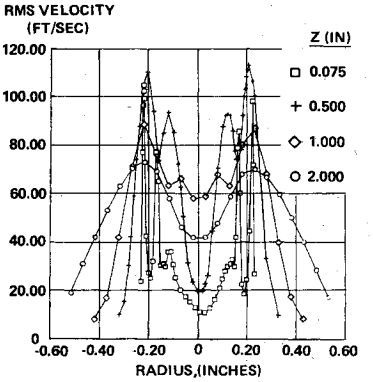

Fig. 11 Comparison of rms velocity profiles for $0.075\leq Z\leq2.0$.

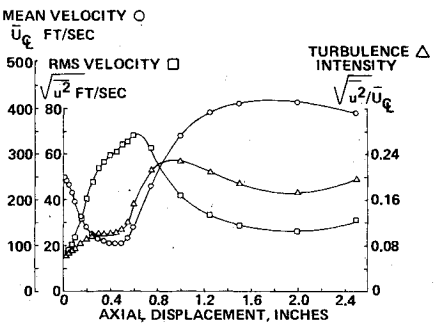

Fig. 12 Comparison of mean velocity and turbulence intensity as function of axial displacement.

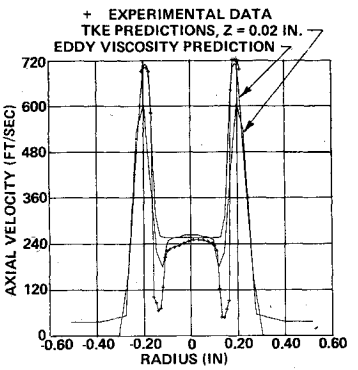

Fig. 13 Comparison of experimental and predicted mean axial velocity profiles, $z=0.030$ in.

with axial displacement. Notice, however, that these regions are different in length as well as being slightly displaced from curve to curve. This is not surprising since turbulence and mean-time scales are different.

Comparison With Analytical Predictions

The ability to make meaningful calculations of turbulent mixing and reacing flows such as those present in modern rockets or chemical lasers has been the goal of many researchers. Such predictions require a detailed understanding of the complex physical processes of turbulent transfer of mass, momentum, and energy and their interactions. Each of these processes are important, however, because of their extreme complexity most turbulent modeling work considers only momentum transport with the assumption that turbulent Schmidt and Prandtl numbers are constant. Assuming that such simplifications are correct and that turbulent mixing alone is the rate controlling process, i.e., the rate of reaction is controlled by the rate of turbulent mixing, there remains the fundamental problem of accurately modeling the momentum transport. There are two approaches generally followed in the

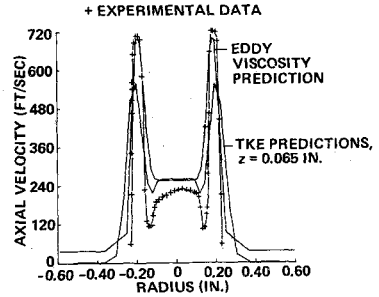

Fig. 14 Comparison of experimental and predicted mean axial velocity profiles, $z = 0.075$ in.

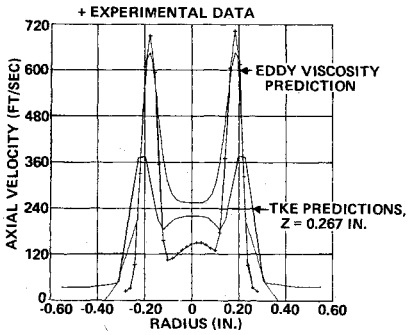

Fig. 15 Comparison of experimental and predicted mean axial velocity profiles, $z = 0.250$ in.

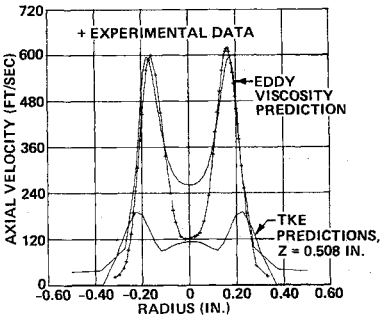

Fig. 16 Comparison of experimental and predicted mean axial velocity profiles, $z = 0.500$ in.

analysis of turbulent flows: the older and most common being to specify an eddy viscosity,[12-14] and the more recent method which introduces one or more additional equations to describe shear stress,[15-19].

Because operational computer programs were available at Bell Aerospace, which used the eddy viscosity model of Ref. 14 and the turbulence kinetic energy approach of Spalding et al.,[18] these specific models were used for prediction of the detailed axial velocity distributions of the coaxial jet for direct comparison with the experimental data. Note that the eddy viscosity model[14] had been specifically developed for predicting axisymmetric coflowing streams and, therefore, was expected to make predictions as accurate as any such model.

The computational technique used for the numerical integration of the continuity, momentum, and energy equations was similar to the method used by Zeiberg and Bleich,[20] i.e., the equations were simplified using boundary layer approximations, the radial velocity was eliminated through use of the von Mises coordinate transformation, and the resulting equations solved by employing an explicit finite difference method. The turbulence kinetic energy (TKE) program and TKE model had been developed by Spalding and coworkers for predicting flows bounded by walls.[18,19] In applying this program to predict coaxial free jet flows, the walls were

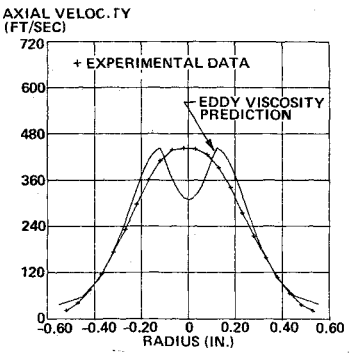

Fig. 17 Comparison of experimental and predicted mean axial velocity profiles, $z = 2.000$ in.

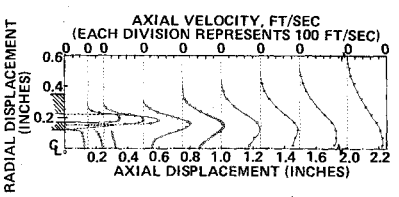

Fig. 18 Coaxial injector flowfield development for $U_0/U_i = 2.5$.

moved from the coaxial element as far as possible to minimize their effect on the computations. The predictive technique used, was to transform the separate conservation equations (mass, momentum and energy) into a "standard" set of nonlinear, elliptic, partial differential equations.[18] The resulting coupled equation set was solved by a finite-difference procedure, using the Gauss-Seidel interactive technique.

Comparison of the predictions obtained with each of these mixing models and the experimental data are presented in Figs. 13-17 For the eddy viscosity model, predictions were available at the identical axial stations for which data were taken; however, because of the aspect ratio constraints of the grid in the "Spalding" analysis, identical stations were not available in all cases. Clearly, the agreement obtained with the TKE model and the data would not have been improved by a minor adjustment of the grid spacing.

Both types of predictions were made assuming initial slug (step) profiles at $z = 0$ using bulk mean velocities. These comparisons demonstrate that neither mixing model is applicable to the coaxial jet flow of this particular coaxial injector. In this particular instance, the eddy viscosity mixing model does a far better job than the TKE model, although the mixing rate is under-predicted somewhat by the eddy viscosity model but drastically overpredicted by the TKE model. Note that neither of the analyses account for the transverse pressure gradients that occur in the actual flow which are in part responsible for their failure to predict the detailed behavior.

Two important features of the eddy viscosity predictions are: 1) The decrease in the central jet velocity at $z < 0.5$ in. is not predicted. Since only momentum transfer between the low-velocity central jet and high-velocity outer jet is considered, no velocities less than that of the original central jet can be computed, and 2) Mixing in the vicinity of the centerline is not sufficiently fast for the velocity maximum to reach the centerline between $z = 1.5$ and 2.0 in. as occurs in the data.

The mixing rates predicted with the TKE model and computational technique designated by Spalding as BRASS are much too fast resulting in very rapid velocity decays. The relative influence of the walls which could not be moved out beyond about 3.5 in. without computational instability resulting, and the influence of the TKE model which overpredicted the mixing drastically could not be assessed.

"Adjustment" of the velocity field, i.e., the profile shapes, no doubt could have been made by further modification of the constants of the models. However, such modification was beyond the scope of this work, which had as its objective an evaluation of existing models. Results clearly demonstrate that a new mixing model, or at least drastic revision of existing models, is required before computation of practical coaxial jet flows in which the velocity of the outer jet is significantly greater than that of the central jet, and which contain a splitter plate, can be made with confidence.

Summary and Conclusions

Static pressure, mean velocity and turbulence intensity profiles in the developing region of a non-reactive (air-air) coaxial jet were presented in which $U_0/U_i = 2.8$, typical of coaxial injector elements. Detailed data were obtained at twelve axial locations (extending from the nozzle exit for a distance of 5 diameters) downstream from a single element of the Bell 19-element coaxial injector. Measurements of mass-flux per unit area (using a constant temperature anemometer), total pressure, and local temperature were used in the determination of local static pressure and velocity.

Figure 18 summarizes in a concise way some of the key features of the velocity field of the injector element. Shown in this figure are measured velocity profiles plotted as a function of distance from the injector exit. Key features illustrated by this two-dimensional representation of the flowfield are: 1) the recirculation zone downstream of the splitter plate, 2) the rapid decrease in velocity of the central jet in the recirculation region owing to both viscous and pressure effects, and 3) the eventual collapsing of the annulus flow around the central jet.

Figures 6 and 7 show the static pressure decreases in the vicinity of the nozzle exit. Although the pressure reduction was only 0.34 psi, it substantially altered the flow. Velocities in the central jet near the nozzle exit decreased initially (there was no central velocity core) as a result of both pressure gradients and viscous mixing.

The experimental results were compared with analytical predictions made using eddy viscosity and turbulence kinetic energy mixing models and available computer codes. Comparisons were disappointing, the eddy viscosity model underpredicted the extent of the mixing, especially in the region within the radius of the central jet; whereas, Spalding's TKE model drastically overpredicted the extent of the mixing throughout the flowfield. In sum, in practical coaxial injectors: 1) The effects of pressure gradients can significantly influence the mixing and combustion, and 2) The turbulence mixing models and computational techniques evaluated do not appear to be adequate for predicting the flow in the developing region of the coaxial jet.

References

[1] Stark, S. B., "Mixing of Gas Streams in a Flame," *Zhurnal Tecknicheskoy Fisiki*, Vol. 23, No. 10, 1953, pp. 1802-1819.

[2] Arutyunov, V. A., "Concerning Mixing Processes in Coaxial Turbulent Streams," *Izvestiya Vysshikh Uchebnykh Zavedeniy*, Vol. 11, 1963, pp. 207-215.

[3] Chigier, N. A. and Beer, J. M., "The Flow Region Near the Nozzle in Double Concentric Jets," *Journal of Basic Engineering*, Transactions of ASME, Series D. Vol. 86, No. 4, Dec. 1963, pp. 797-804.

[4] Champagne, F. H. and Wyganski, I. J., "An Experimental Investigation of Co-Axial Jets," *International Journal of Heat and Mass Transfer*, Vol. 14, 1971, pp. 1445-1464.

[5] Durao, D., and Whitelaw, J.H., "Turbulent Mixing in the Developing Region of Coaxial Jets," ASME Paper 73-FE-19, June 1973.

[6] Morgenthaler, J. H., Moon, L. F., and Stepien, W. R., "Developing a Gas Rocket Performance Prediction Technique," NAS3-16798, Oct. 28, 1974.

[7] "Hydrogen-Oxygen APS Engines, Volume I: High Pressure Thruster," Rocketdyne Final Report, Feb. 1973, Canoga Park, Calif., NASA, CR-120805 (R-8837-1), Feb. 1973.

[8] "Hydrogen-Oxygen Auxiliary Propulsion for the Space Shuttle, Volume I: High Pressure Thrusters," Aerojet Liquid Rocket Company Final Rept., 30, Jan. 1973, Sacramento, Calif., NASA, CR-120895.

[9] "High Pressure Reverse Flow APS Engine," Bell Aerospace Report 8636-950004, Nov. 1972; NASA CR 120881, Nov. 1972, Buffalo, New York.

[10] Hinze, J. O., *Turbulence*, McGraw-Hill, New York, N. Y., 1959.

[11] Ricou, F. D. and Spalding, D. B., "Measurements of Entrainment of Axisymmetrical Turbulent Jets," *Journal of Fluid Mechanics*, Vol. 11, No. 21, Aug. 1961, pp. 21-32.

[12] Edelman, R.B. and Fortune, O.F., "An Analysis of Mixing and Combustion in Ducted Flows," AIAA Paper 68-114, New York, N. Y., 1968.

[13] Peters, C. E., Phares, W. J., and Cummingham, T. H. M., "Theoretical and Experimental Studies of Ducted Mixing and Burning of Coaxial Streams," AIAA Paper 69-85, New York, N. Y., 1969.

[14] Zelazny, S. W., Morgenthaler, J. H., and Herendeen, D. L., "Shear Stress and Turbulence Intensity Models for Coflowing Axisymmetric Streams," *AIAA Journal*, Vol. 11, Aug. 1973, pp. 1165-1173.

[15] Bradshaw, P., Ferris, D. H., and Atwell, N. P., "Calculation of Boundary-Layer Development Using the Turbulent Energy Equation," *Journal of Fluid Mechanics*, Vol. 28, No. 3, 1967, pp. 593-616.

[16] Lee, S. C. and Harsha, P. T., "The Use of Turbulent Kinetic Energy in Free Mixing Studies," AIAA Paper 69-683, Princeton, N. J., 1969.

[17] Donaldson, C. duP. and Rosenbaum, H., "Calculation of Turbulent Shear Flows Through Closure of the Reynolds Equations by Invarient Modeling," ARAP Inc., Rept. 127, Dec. 1968, Princeton, N.J.

[18] Gosman, A. D., et al., *Heat and Mass Transfer in Recirculating Flow*, Academic Press, London, 1969.

[19] Launder, B. E., Morse, A., Rodi, W., and Spalding, D. B., "Prediction of Free Shear Flows—A Comparison of the Performance of Six Turbulent Models," *Free Turbulence Shear Flows*, Vol. I—Conference Proceedings, pp. 361-422, NASA, SP-321, July 1972.

[20] Zeiberg, S. L. and Bleich, G. D., "Finite Difference Calculations," *AIAA Journal*, Vol. 2, 1964, pp. 1396-1402.